Journal of Research in Pharmacy

Research Article

www.jrespharm.com

Design and Characterization of Transethosomes loaded with Rivastigmine for Enhanced Transdermal Delivery

Cynthia Lizzie LOBO[1] Sneh PRIYA[1]*

[1] Department of Pharmaceutics, NGSM Institute of Pharmaceutical Sciences, Nitte (Deemed to be University), Mangalore, India.

* Corresponding Author. E-mail: snehpriya123@nitte.edu.in (S.P.); Tel. +91-9916988245.

Received: 17 July 2023 / Revised: 24 August 2023 / Accepted: 31 August 2023

ABSTRACT: This research aimed to create and optimize a transethosomal patch containing Rivastigmine Hydrogen Tartarate, a cholinesterase inhibitor, for the symptomatic management of Alzheimer's disease that would reduce drug loading and patch size. Transethosomes are elastic vesicles made up of phospholipids, ethanol, and edge activator. Transethosomes of Rivastigmine were prepared by cold method, which were then incorporated into a transdermal adhesive patch prepared by solvent casting method. The transethosomes were optimised using the central composite design. The optimized transethosomes showed low vesicle size, good entrapment efficiency and enhanced transdermal flux. The electron microscopy revealed that the vesicles were uniform and sphere-shaped, also the vesicle surface was found to be smooth. Rivastigmine Hydrogen Tartarate was released slowly in the study, and the mechanism of drug release followed the Korsemeyer-Peppas model. Transethosomal formulation showed significant increase in the steady state flux to 2.18 times than the pure drug solution. Also, the transethosomal patch showed significant increase in the steady state flux to 1.55 times than the conventional patch. Based on the results, Rivastigmine Hydrogen Tartarate loaded transethosomal patch was the best formulation since it provided long-term drug release.

KEYWORDS: Rivastigmine; transdermal route, transethosomes; Alzheimer's disease; patch.

1. INTRODUCTION

Alzheimer's disease is a neurological disease that progresses over time. It is irreparable and entails the gradual degradation of neurons involved in learning and memory functions [1]. It is responsible for 60-70% of dementia cases. Cholinesterase inhibitors (Rivastigmine, Donepezil, Galantamine) and N-methyl-D-aspartate (NMDA) receptor antagonists (Memantine) have been licenced by the USFDA to treat Alzheimer's disease cognitive symptoms. In Alzheimer's disease the amount of acetylcholine available to carry messages is less due to the damaging or destruction of cells that produce and use acetylcholine. A cholinesterase inhibitor inhibits the activity of acetylcholinesterase, reducing acetylcholine breakdown. By maintaining acetylcholine levels in the brain, the medication may help compensate for the loss of functioning brain cells [2]. Rivastigmine is approved to treat Alzheimer's disease in people who have mild to moderate symptoms.

Alzheimer's disease is treated using pharmaceutical formulation such as capsules, oral solutions, and transdermal patches. Anti-alzheimer medicines used orally have a low bioavailability and have adverse effects such as nausea, vomiting, renal failure, hepatotoxicity, and malaise, which can lead to the patient discontinuing treatment [3]. Transdermal route for drug delivery reduces the side effects oral administration of the drug and providing easy accesses to therapeutically effective doses thus improving patient compliance [4]. A study suggests that Rivastigmine transdermal patch provides an effective long-term management of Alzheimer's disease when compared to oral Rivastigmine capsules [5]. In 2007, the rivastigmine transdermal patch, the first of these therapies, became accessible in a number of countries. According to pharmacokinetic studies, approximately half of the total dose put into the patch of rivastigmine gets absorbed into the bloodstream over the course of 24 hour [3]. The major drawback of transdermal delivery is poor permeability of the skin due to the presence of stratum corneum which has a barrier function and only those drug molecules that are small in size to penetrate the skin can be administered by transdermal route and skin irritation may occur due to the excipients and the penetration enhancers incorporated in the drug delivery system and also it may be uncomfortable to wear the patch [6]. Also due to the hydrophilic nature of rivastigmine absorption through the skin may be incomplete or difficult due to

How to cite this article: Lobo CL, Priya S. Design and Characterization of Transethosomes loaded with Rivastigmine for Enhanced Transdermal Delivery. J Res Pharm. 2024; 28(5): 1409-1422.

ISSN: 2630-6344

http://dx.doi.org/10.29228/jrp.819

limitations of partitioning into the stratum corneum. Therefore, it is necessary to formulate novel lipid vesicle systems such as liposomes, transferosomes, ethosomes, transethosomes etc. loaded with rivastigmine for transdermal delivery. Various formulations of Rivastigmine Hydrogen Tartarate such as liposomes [7], polymeric nanaoparticles [1,8], nanolipid carrier loaded transdemal pacthes [9] have been reported. Meenakshi et al. developed nanolipid carrier (NLC) loaded transdermal system of rivastigmine for bioavailability enhancement which showed sustained drug release in comparison to conventional patch. Transethosomes are phospholipid, ethanol and edge activators (surfactant) containing elastic vesicles. Depending on the drug, the size range varies 40 nm to 200 nm [10]. Song et al. first introduced transethosomes in 2012. Transethosomes are found to be irregularly spherical shaped and possess higher vesicle elasticity as well as skin permeation. This could be owing to the combination of ethanol and edge activator causing lipid bilayer rearrangement in these vesicles. Transethosomes ensure increased drug permeation through the skin. This eliminates presystemic metabolism.

Rivastigmine undergoes significant first-pass metabolism which results in its lower oral bioavailability (36%). It has a short elimination half-life of approximately 1hr. Thus, the transdermal route is the best for rivastigmine as it has low molecular weight (250.3 D), optimum log P value (3.0) and low dose. It is extremely soluble in water, soluble in ethanol, and acetonitrile, but only marginally soluble in n-octanol and ethyl acetate.

Rivastigmine is only symptomatic and not a causal treatment of Alzheimer's disease [11]. The maximum plasma peak of the drug was seen within 1 hour of oral administration of the rivastigmine capsule. Nausea and vomiting occur more frequently in patients as the level of drug increases in plasma, Rivastigmine plasma levels rise more slowly after patch application, reaching their maximal level after about 8 hours. However a matrix type of transdermal patch of Rivastigmine Hydrogen Tartarate, Exelon® is available in the market with an initial dose of 4.6 mg/ 24 hrs. It has been reported that 9 mg of drug has been loaded into a patch of 5 cm^2, out of which only 4.6 mg of the drug has been diffused from the patch at the end of 24 hrs. With the rivastigmine patch, gastrointestinal side effects are considerably reduced due to the smoother, more constant drug delivery. Patients switching from oral rivastigmine towards the rivastigmine patch had nausea in upto 3.2% and vomiting in upto 1.9% of cases [3]. The rational strategy adopted was to incorporate the drug in sustained release formulations such as those that may reduce the fluctuations in serum drug level. Further release and pharmacokinetics of the drug can be improved by incorporating the drug-loaded transethosomes in a transdermal patch.

2. RESULTS AND DISCUSSION

2.1. Design of Experiments

RHT-loaded transethosomes were formulated by the cold method as per the central composite design. The effect of soya lecithin as well as ethanol concentration on the responses such as vesicle size, PDI and entrapment efficiency, were statistically analysed by using design expert software and the results were shown in Tables 2 and 3.

2.1.1. Vesicle size of transethosomes

Vesicle size has a crucial role in skin permeation of transethosomes as per the literature reported. The independent variables i.e., the concentration of soya lecithin and concentration of ethanol exhibited significant effects on the vesicle size as illustrated in the 3D graph (Figure 1A & Table 1). The Central Composite Design showed that increase in soya lecithin concentration from 0.5 to 2% w/v, there was increase in the vesicle size at all concentrations of ethanol, as phospholipids are the main constituents of transethosomes and also soya lecithin has a cylindrical form due to the bulky volume of its hydrophobic tail [12]. As the ethanol concentration increased from 20 to 40% v/v initially showed a decrease in the vesicle size upto certain concentration and then the vesicle size increased at all concentrations of soya lecithin. The size of transethosomes reduces due to the reduction in the thickness of the membrane and also owing to the formation of a phase with interpenetrating hydrocarbon chains [13]. As shown in Table 2, the p-value for the vesicle size model was less than 0.05, and the F value was 19.23, showing that the Quadratic model was significant. The value of 3.48 indicates a non-significant lack of fit, indicating that the model is suitable for determining vesicle size. The Predicted R^2 of 0.7548 is in reasonable agreement with the Adjusted R^2 of 0.8836; i.e. the difference is less than 0.2. The polynomial equation derived from the analysis results:

$$\text{Vesicle Size} = +140.94 + 22.38(A)^* - 9.89(B)^* - 10.42(AB)^* + 6.12(A^2) + 9.39(B^2)^*$$

Where A is the concentration of soya lecithin, B is the concentration of ethanol, the coefficient in this equation reflects the standardized beta coefficient and the asterisk symbol implies variable significance. A synergistic effect is represented by a positive sign, while an antagonistic effect is represented by a negative sign. From the polynomial equation it is clear that an increase in the concentration of soya lecithin increases the vesicle size, whereas, in the case of ethanol, the vesicle size was found to decrease as the concentration of ethanol increased, which is similar to results obtained for transethosomal gel system of Piroxicam [14].

2.1.2. PDI of transethosomes

The width of unimodal size distributions is measured using PDI. A value of 0 denotes homogenous dispersion, whereas a value of 1 suggests a completely heterogeneous polydisperse population. A PDI of 0.5 or less is considered acceptable. The concentration of soya lecithin and ethanol displayed significant effects on PDI as represented in the 3D graph (Figure 1B and Table 1). The p-value for the PDI model was less than 0.05, and the F value was 4.93, showing that the Quadratic model was significant. The value of 4.26 indicates that the lack of fit is not significant, showing that the model is suitable for calculating the PDI. A negative Predicted R^2 infers that the overall mean may be a better predictor of the response. This could be because the studied factors did not affect the PDI of the prepared transethosomes which was also reported for transethosomes loaded with olmesartan medoxomil [15]. The polynomial equation derived from the analysis result:

$$PDI = + 0.5254 + 0.0139\ (A) + 0.0314\ (B)^* - 0.0257\ (AB) - 0.0218\ (A^2) - 0.0096\ (B^2)$$

Where A is the concentration of soya lecithin, B is the concentration of ethanol, the coefficient in this equation reflects the standardized beta coefficient and the asterisk symbol implies variable significance. The polynomial equation shows that there is a positive effect of ethanol concentration on the PDI. However, there was not much effect of the factors on the PDI of the formulation.

2.1.3. Percentage entrapment efficiency

The 3D Response surface graph (Figure 1C and Table 1) displays that an increase in soya lecithin concentration also increases the entrapment efficiency of the drug, as soya lecithin is a vesicle-forming agent, more vesicles are formed and hence more drug is entrapped. After an initial increase in ethanol concentration, the entrapment efficiency gradually decreases. The initial increase in the entrapment efficiency is due to ethanol which increased the membrane's fluidity. Furthermore, as the ethanol concentration increased, the entrapment efficiency decreased, making the vesicle membrane leaky [16]. The p-value for the entrapment efficiency model was less than 0.05, and the F value was 20.69 showing that the Quadratic model was significant. The model is appropriate to determine the entrapment efficiency because the value of 1.10 shows a non-significant lack of fit. The adjusted R^2 of 0.8913 is close to the predicted R^2 of 0.7418; the difference is less than 0.2. The polynomial equation derived from the analysis results:

$$EE = + 62.87 + 9.86\ (A)^* + 0.9945\ (B) + 1.88\ (AB) - 5.20\ (A^2)^* - 9.57\ (B^2)^*$$

Where A is the concentration of soya lecithin, B is the concentration of ethanol, the coefficient in this equation reflects the standardized beta coefficient and the asterisk symbol implies variable significance. The polynomial equation shows the positive effect of soya lecithin concentration on entrapment efficiency which is similar to reported letertaure [14].

2.1.4. Optimization of transethosomes loaded with RHT

The optimum formulation of transethosome was selected by applying constraints on the dependent factors, as shown in Table 1. The predicted values given by software for vesicle size, PDI and % EE of the optimized formulation are 132.127, 0.482, and 51.97 %, respectively, whereas the experimental value obtained were 129.3nm, 0.478 and 52.38 %. That is in good agreement with the predicted values generated by the software, i.e., within ± 5% error, and the result assures the validity of the RSM model.

Journal of Research in Pharmacy
Research Article

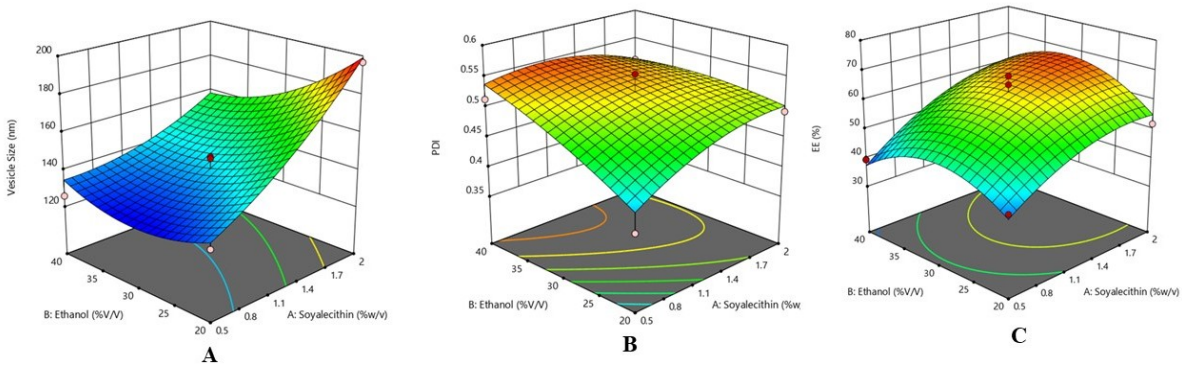

Figure 1. Response surface curve representing the effect of Soya lecithin and Ethanol on the A) vesicle size B)PDI C) Entrapment efficiency of transethosomes.

Table 1. Composition and response of transethosomes as per Central Composite Design.

Formulation Code	Soya lecithin %w/v: A	Ethanol concentration %v/v: B	Vesicle Size nm Y_1	PDI Y_2	Entrapment Efficiency %, Y_3
F1	1.25	15.8579	175.4± 2.33	0.484	43.20± 1.75
F2	2	20	196.7± 1.98	0.493	51.95± 2.01
F3	1.25	44.1421	155.3± 4.21	0.562	45.29± 1.39
F4	1.25	30	146.3± 2.54	0.517	59.04± 2.91
F5	2	40	150.5± 3.81	0.512	58.21± 1.72
F6	0.5	40	125.8± 4.19	0.513	39.45± 2.83
F7	1.25	30	137.7± 3.37	0.514	61.54± 1,95
F8	1.25	30	134.8± 2.85	0.554	65.29± 2.63
F9	1.25	30	138.7± 2.92	0.523	68.26± 3.03
F10	0.18934	30	127.7± 4.05	0.495	35.72± 2.63
F11	2.31066	30	189.9± 4.02	0.502	70.29± 1.93
F12	0.5	20	130.3± 2.41	0.391	40.76± 3.02
F13	1.25	30	147.2± 3.03	0.519	60.29± 2.65

mean± SD (n=3)

2.2. Characterization of RHT-loaded transethosomes

2.2.1. Zeta potential of optimized formulation

The zeta potential of the optimized formulation was -29.4 mV. As ethanol and sodium deoxycholate were present, the zeta potential of transethosomes was negative [16]. The charge of transethosomes is a significant factor that affects both vesicular attributes like stability and skin-vesicle interactions.

2.2.2. Scanning electron microscopy & Transmission Electron Microscopy

The surface morphology and vesicle size of the formulated transethosomes are obtained using SEM. The image is shown in Figure 2. Vesicles were discovered to be round, homogeneous, and smooth on the surface. SEM analysis also supported that the vesicle size was less than 200 nm. The TEM photographs given in Figure 3 showed the surface morphology of vesicles with the presence of a unilamellar vesicular structure.

2.2.3. In vitro drug release studies of formulations

The in vitro drug release profile of different formulations and the pure drug is represented in Figure 4. By this, we can infer that the encapsulation of Rivastigmine Hydrogen Tartrate into transethosomes resulted in prolonged release [16] across the dialysis membrane in comparison with the pure drug solution,

liposomes and ethosomes. A sustained effect was observed in the order: transethosomal suspension > ethosomal suspension > liposomal suspension > pure drug solution.

Table 2. Summary of Regression analysis and ANOVA.

Sl. No.	Factor	Vesicle size (Adjusted R^2 = 0.8836)		PDI (Adjusted R^2 = 0.8208)		% EE (Adjusted R^2 = 0.8913)	
		β coefficient	P-value	β coefficient	P-value	β coefficient	P-value
1.	Intercept	140.94	0.0006	0.5254	0.0298	62.87	0.0005
2.	A-Soya lecithin	22.38	< 0.0001*	0.0139	0.1645	9.86	0.0002*
3.	B-Ethanol	-9.89	0.0095*	0.0314	0.0098*	0.9945	0.4909
4.	AB	-10.42	0.0336*	-0.0257	0.0808	1.88	0.3647
5.	A^2	6.12	0.0806	-0.0218	0.0567	-5.20	0.0094*
6.	B^2	9.39	0.0165*	-0.0096	0.3506	-9.57	0.0003*

*Statistical significance of independent variables.

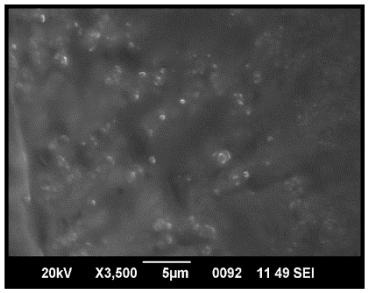

Figure 2. SEM image of RHT transethosomes.

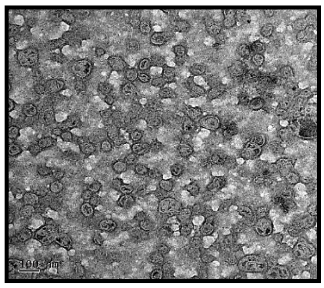

Figure 3. TEM image of RHT transethosomes.

2.2.4. In vitro drug release kinetics

Various kinetic models analysed the release kinetics of different formulations and pure drugs. The data analysis was focused on the corresponding significance of the regression coefficients. The optimized transethosomal, liposomal, and ethosomal suspension followed the first-order release kinetics whereas the pure drug solution followed zero-order kinetics. The mechanism involved in the drug release from the nano-vesicles was studied by fitting the data to the Higuchi model and Korsemeyer-Peppas exponential model. Good linearity was observed for all the formulations with a larger regression coefficient. The release exponent (n) of transethosomes, liposomes and ethosomes was found to be beyond 0.45 which indicates that the release is defined by Non-Fickian diffusion, which could mean that more than one process regulates the release rates of drugs, i.e. diffusion coupled with erosion mechanism.

2.2.5. Ex vivo drug permeation studies of formulations

Ex vivo study has been performed to determine the amount of drug permeated through the porcine ear skin. The obtained release profile is represented in Figure 5. The permeation of transethosomes is much more enhanced than the pure drug solution. Phospholipid vesicles, ethanol, and skin lipids have a synergistic mechanism. Ethanol causes fluidization of the stratum corneum lipids which enhances drug permeation. Ethanol also increases the lipid fluidity of lipid carriers thus making them more flexible. These flexible vesicles squeeze through the disturbed stratum corneum into the deeper layers of skin, releasing the medicament by the fusion of transethosomes with skin lipids [17]. The order of permeation profile observed was: transethosomes > ethosomes > liposomes > pure drug solution.

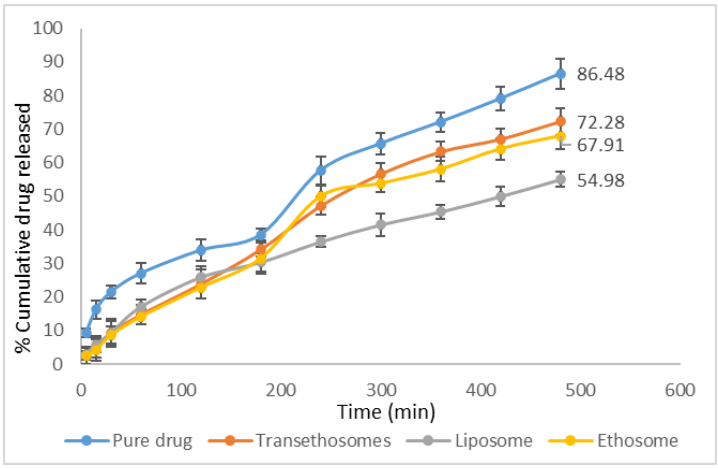

Figure 4. The comparative *in vitro* drug release profile of RHT, transethosome, liposome and ethosome.

The steady-state flux was found to be highest for transethosomes as shown in Table 3. Higher flux, as well as release, was observed for transethosomes in comparison to pure drug solution owing to the synergistic mechanisms of ethanol, phospholipid vesicles, edge activator as well as the skin lipids interaction [18], which enhanced the passage of Rivastigmine Hydrogen Tartrate through the porcine ear skin.

2.2.6. Elasticity test

Transethosomes were found to have a higher deformability index as shown in Table 3, than the ethosomes and liposomes. Transethosomes are highly elastic in nature and the presence of ethanol as well as sodium deoxycholate, an edge activator imparts higher deformability to transethosomes compared to ethosomes which are devoid of edge activator and liposomes which do not contain ethanol [19].

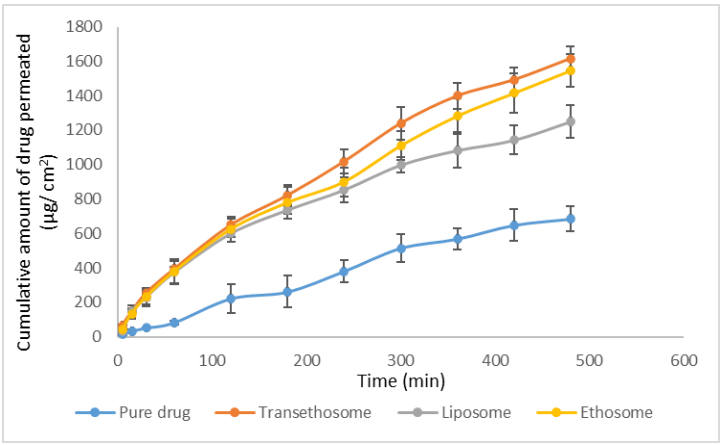

Figure 5. *Ex vivo* permeability profile of RHT, transethosome, liposome and ethosome.

2.3. Formulation and evaluation of patch incorporated with RHT-loaded transethosomes

RHT-loaded transethosomal patches (Figure 6) were prepared by solvent casting method. The prepared patches were smooth, flexible and uniform in thickness and appearance.

2.3.1. Drug content

The drug content of the conventional and transethosomal patches was found to be 1.73 ± 0.13 mg/cm² and 1.62 ± 0.11 mg/cm², respectively. The standard deviation was found to be very less, ensuring good uniformity of drug in the patch.

2.3.2. Compatibility study of drug-excipient by FT-IR

The major IR peaks of the pure drug and optimized transethosomal patch are given in Table 4. The principle peaks of the drug were present in the final formulations, which indicates compatibility between the drug and the excipient used.

Table 3. Permeation parameter of vesicular formulation and their deformability index.

Form. Code	Permeated amount at 480 mins (µg/cm²)	Flux (µg/cm². min)	Permeability constant (K_p) × 10^{-3} (cm/h)	Deformability Index (ml/s)
Pure drug	688.18	1.5072	0.3768	-
TE	1624.54	3.2891	0.8222	13.45
L	1249.31	2.449	0.6122	1.06
E	1545.68	3.0785	0.7696	7.12

* TE – transethosomes, L – liposome, E – ethosomes.

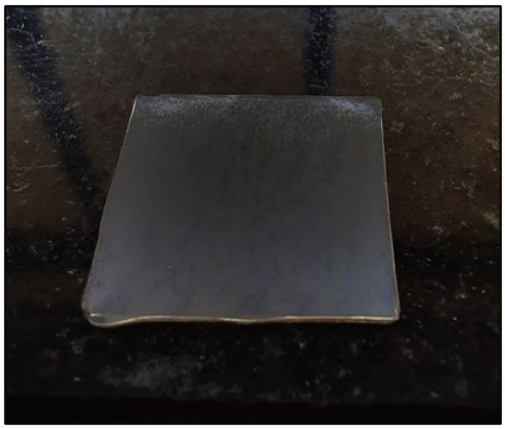

Figure 6. RHT-loaded Transethosomal patch.

Table 4. Major IR peaks of pure rivastigmine hydrogen tartrate and optimized transethosomal patch.

Samples	Composition	Major Peaks (wave numbers cm^{-1})
A	Pure Rivastigmine Hydrogen Tartarate	3415.47, 2942.61, 1691.90, 1156.72, 1227.19, 1008.56.
B	Optimized Transethosomal Patch	3363.27, 2938.70, 1738.32, 1139.20, 1241.50, 1076.10.

2.3.3. Ex vivo drug permeation studies of patches

An *Ex vivo* study has been performed to determine the amount of drug permeated through the porcine ear skin. The obtained release profile is shown in Figure 7. There was higher drug permeation in case of the transethosomal patch than the conventional patch as the hydrophilic drug, Rivastigmine Hydrogen Tartrate was encapsulated within the transethosomes which imparted a lipophilic nature which is a prerequisite for a molecule to cross the biological membrane. In addition, the permeation profile of the transethosomal patch indicated a slow release compared to transethosomal suspension as in the case of the transethosomal patch, the nano-vesicle has to first diffuse from the patch matrix, followed by diffusion of RHT through the nano-vesicle in which it is entrapped. The steady-state flux was higher for the transethosomal patch than the conventional patch as shown in Table 5. Also, the permeability coefficient of the transethosomal patch was higher than the conventional patch. The results could be attributed to the higher deformability and flexibility of transethosomes, which enabled them to overcome the skin barrier challenges. Albash et al. reported similar results in their research work in which transethosomal gel was investigated as a carrier for transdermal delivery of olmesartan medoxomil [15]. The study performed by Albash et al. and our work revealed that transethosomes can be skin permeation enhancers for hydrophilic drugs like RHT and olmesartan medoxomil.

2.3.4. Skin deposition studies

Higher skin deposition of transethosomal patch than conventional patch was obtained as shown in Table 5, as a result of the combined effect of a phospholipid, edge activator as well as ethanol on the skin, thus acting as a depot and providing an approach for sustained delivery of drug for a longer duration. Allam et al. formulated transethosomes loaded with minoxidil which also showed higher skin deposition in comparision to drug solution [20]. Therefore, hydrophillic drugs such as RHT and minoxidil can be better retained in the skin by encapsulting these hydrophillic drugs into tranesthosomes.

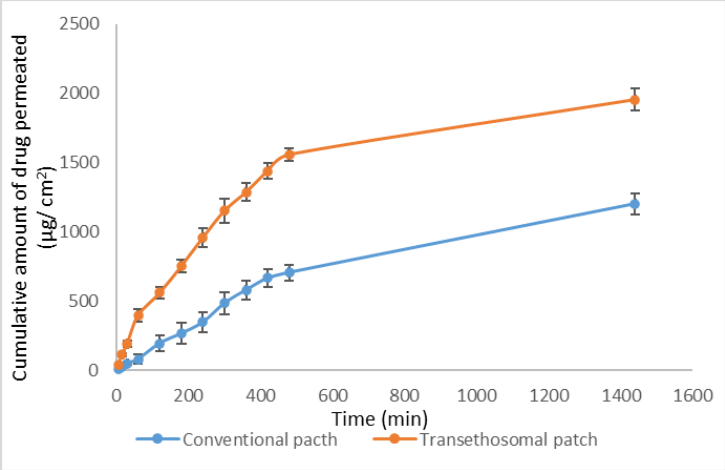

Figure 7. Ex vivo drug permeation profile of conventional patch and transethosomal patch.

Table 5. Permeated amount of rivastigmine hydrogen tartrate at 1440 mins, flux, permeability coefficient and amount of drug deposited in the skin from patches.

Form. Code	Permeated amount at 1440 mins (µg/cm²)	Flux (µg/cm². min)	Permeability constant (K_P) × 10^{-3} (cm/h)	Amount of drug deposited in the skin (µg/cm²)
CP	1202.5	0.8618	0.2364	168.79
TEP	1955.45	1.3417	0.3680	230.34

*CP – conventional patch, TEP – transethosomal patch.

2.4. Comparative studies of developed patches with the marketed patch

The marketed patch is available as 5 cm² and 10 cm² transdermal patches containing 9 mg and 18 mg of Rivastigmine Hydrogen Tartrate. The comparative drug loadings and sizes of marketed and developed patches were given in Table 6. Moreover, the developed transethosomal patch contains a drug entrapped within the transethosome which helps the drug permeate more than the marketed patches and conventional patches, it could be due to alterations in the physico-chemical properties of a drug. This supports lesser Rivastigmine loading and small sized transethosome loaded patches. From the above result, it can be concluded that the developed patch of drugs loaded in transethosomes can be a potential alternative to the existing marketed patch.

Table 6. Comparative deatil of drug loadings and sizes of marketed and developed patch

Product	Total area (cm²)	The total drug in a patch (mg)	Amount / 24 h
Marketed patch	5	9	4.6
CP	5.04	9.07	4.6
TEP	3.30	5.94	4.6

* CP – Conventional patch, TEP – Transethosomal patch.

3. CONCLUSION

Transethosomes grafted with Rivastigmine Hydrogen Tartrate were fabricated as a drug-in-adhesive patch. Using Design Expert software, the response obtained for 13 runs was subjected to multiple regression analysis. The transethosomes were optimized based on the responses with minimum vesicle size, with minimum PDI and maximum entrapment efficiency. The observed values for vesicle size, PDI and entrapment efficiency were found to be 129.3 nm, 0.478 and 52.38% respectively; which were within 95% of CI of the predicted value which is acceptable. The images obtained from optical microscopy, scanning electron microscopy and transmission electron microscopy indicated that the transethosomes formed were smooth, spherical and having uniform size with a vesicle size less than 500nm. The transethosomal patch showed a significant increase in the steady state flux and permeability coefficients to 1.55 times that of the conventional patch containing a pure drug. The evaluation studies showed that these transethosomal patches could be a promising formulation in the transdermal delivery of Rivastigmine Hydrogen Tartrate in the symptomatic treatment of Alzheimer's disease. Future in vivo bioavailability studies can be conducted for a better understanding of the ability of transethosomal patches to surpass the barrier properties of the skin and better management of dementia in Alzheimer's disease.

4. MATERIALS AND METHODS

4.1. Materials

Rivastigmine hydrogen tartrate (RHT) was obtained from Yarrow chem products (Mumbai, India). Soya lecithin was obtained from Hi Media laboratories (Mumbai, India). Ethanol was obtained from Nice Chemicals (Kerala, India). Eudragit E 100 was obtained from Yarrow chem products (Mumbai, India). Dibutyl sebacate was procured from Merck (Mumbai, India). Succinic acid was obtained from Reachem Laboratory Chemicals (Chennai, India). All other reagents were of analytical grade.

4.2. Methods

4.2.1. Formulation of transethosomes - Design of Experiments

DoE is a well-design and systematized procedure for analysing the links between input variables (independent variables) and output responses using mathematical models. The literature survey suggested the two independent variables, soya lecithin concentration (A) and ethanol concentration (B) [21,22] and their possessions were evaluated on three dependent variables including vesicle size, PDI and entrapment efficiency of transethosomes. The developed transethosomal preparations were optimized by using "Central Composite Design" with 5 center points by the "Design Expert ® software (version 11.0.3.0 64-bit, Stat- Ease, Inc. Minneapolis, MN, USA)". A numeric factor is set to 5 levels: plus and minus alpha (axial points), plus and minus 1 (factorial points) and the centre point. The transethosomes were prepared by considering the two independent variables [soya lecithin (%w/v) and ethanol (%v/v)] at different levels. For optimizing the transethosomal formulation the concentration of soya lecithin and ethanol were varied as shown in Table 1. The design presented an overall of 13 formulation runs as shown in Table 1.

Table 7. Factors and levels

Levels			Dependent Variables	Desirability
Independent Variables	**Low**	**High**		
Soya lecithin (X1, %w/v)	0.5	2	Vesicle size (Y1, nm)	Minimum
Ethanol (X2, %v/v)	20	40	PDI (Y2)	Minimum
			EE (Y3, %)	Maximum

4.2.2. Preparation of transethosomes

Transethosomes loaded with Rivastigmine Hydrogen Tartrate were prepared by cold method as per Table 1. 80 mg of Soya lecithin and 3 ml of 30% v/v of ethanol were stirred for 15 minutes on a magnetic stirrer (Remi, 1MLH), at 700 rpm by maintaining 30˚C with the help of a water bath. An aqueous phase composed of 20 mg of drug and 15 mg of Sodium deoxycholate dissolved in Phosphate buffer pH 7.4 was introduced into the organic phase in a fine stream. For another 5 minutes, the mixture was stirred. After that, the product was sonicated for 10 minutes with an ultrasonic probe sonicator (Sonics Vibra cell, CV18) [16].

Formulation of an optimized batch of transethosomes - The effect of process variables on the responses was evaluated dynamically by applying one-way ANOVA, using the commercially accessible software program Design-Expert version 11, to refine the parameters for the formulation. The transethosome was optimised by providing Constraints such as particle size and PDI minimum and percentage entrapment efficiency maximum. The software provided a solution that was chosen based on desirability near one. The optimal formulation is comprised of 0.748% w/v soya lecithin and 25.32% v/v ethanol, as per the software's solution. The optimised batch was created in the same manner as the other batches.

Similarly, the Rivastigmine Hydrogen Tartrate liposomes were prepared using the same method without the addition of Ethanol and the ethosomes were prepared without the addition of Sodium deoxycholate.

Rivastigmine Hydrogen Tartarate ethosomes were prepared by cold method as mentioned above without the addition of Sodium deoxycholate. Rivastigmine Hydrogen Tartrate liposomes were prepared by the lipid layer hydration method. Software suggested composition of soya lecithin and cholestrol were dissolved in chloroform and transferred in 100 mL round bottom flask which was attched to a Rotary evaporator (Rotavap, PBU-6D) immersed in 45°C water bath and rotated under vacuum pump until a dry thin lipid film was formed. RHT was dissolved in phosphate buffer saline pH 7.4 and added to the dried film for rehydration. On complete rehydartion of the lipid film, the liposome suspension was sonicated for 10 minutes with an ultrasonic probe sonicator (Sonics Vibra cell, CV18) [7].

4.2.3. Characterization of RHT-loaded Transethosomes

Vesicle size, size distribution and zeta potential - The Zeta sizer (Nano ZS, Malvern Instruments, UK) was utilised to measure the vesicle size and size distribution of transethosomes using dynamic light scattering.The overall charge that particles acquire in a given medium is known as Zeta potential. The values of zeta potential are used to determine the formulation's stability [23].

Percentage of drug entrapment efficiency - 10 ml of transethosomal suspension was centrifuged for 60 minutes at 12,000 rpm & 4°C in a 15 ml Tarsons centrifuge tube. Centrifugation separates the supernatant from the sediment. The UV spectroscopic approach was used to determine the concentration of Rivastigmine Hydrogen Tartrate in the supernatant at 263 nm. The following formula was used to determine the percentage entrapment efficiency [24].

$$\% \text{ Entrapment efficiency} = \frac{\text{Amount of entrapped drug}}{\text{Total amount of drug}} \times 100$$

Scanning Electron Microscopy (SEM) - A morphological study of Rivastigmine Hydrogen Tartarate loaded transethosomes can be done using Scanning Electron Microscopy. A drop of the transethosomal formulation was placed on a glass stub and allowed to dry naturally and then examined using a scanning electron microscope [21].

Transmission Electron Microscopy (TEM) - Surface appearance and shape of vesicles is determined using Transmission Electron Microscopy. Transethosomal suspension is dispersed in distilled water and then 10 µL of this diluted suspension was located on carbon coated grid which was then visualized using Jeol/JM 2100, source LaB6 electron microscope. In the process described above, a 200 kV accelerating voltage is used [25,26].

In vitro drug release studies of formulations - The release study of the drug was performed by Franz diffusion cell. It has two compartments. The donor compartment has two open ends, one of which is covered with a cellophane membrane that has been soaked in phosphate buffer pH 7.4. On each cellophane membrane, equivalent to 4 mg of the drug in solution, transethosomal, liposomal, and ethosomal suspension was placed. In the reservoir compartment, filled with 12 ml of buffer, a small magnetic bead rotated at a constant speed of 50 rpm. The experiment took place for 8 hours at 37± 0.5°C. 1 ml of samples were taken from the reservoir compartment and diluted, and the absorbance was measured spectrophotometrically at 263 nm at a predetermined time interval. To maintain the sink condition, the reservoir compartment is supplied with the same amount of fresh phosphate buffer at pH 7.4 [27].

Drug release kinetics - The data from the drug release experiment was analysed using zero-order (% CDR versus time), first-order (cumulative percentage of drug remaining versus time). Fitting to the Korsemeyer-Peppas (log %CDR vs log time) and Higuchi matrix models determine the mechanism of drug release (% CDR vs square root of time).

Ex vivo drug permeation studies of formulations - Since the porcine ear skin is relatively thin and highly vascularized, it has been employed as a predictive model because it is the best alternative to human

skin. The porcine skin lipid composition was also found to be comparable to that of human skin [28,29]. As a result, the current study used porcine ear skin as an ex vivo model for human skin. Fresh pig ears were gotten from a local slaughterhouse and thoroughly cleaned to achieve hairless skin before being stored in phosphate buffer pH 7.4. Two compartments containing Franz Diffusion cells were used in the ex vivo skin experiments. On each dermal side of the skin, 0.4 ml of pure drug solution (equal to 4 mg of drug) and 0.3 ml of transethosomal, liposomal, and ethosomal suspension (equivalent to 4 mg of drug) were deposited in the donor compartment. The reservoir compartment was filled with 12 ml of pH 7.4 phosphate buffer and a small rotating magnetic bead that rotated at a constant 50 rpm. The experiment lasted 8 hours at 37± 0.5 °C. 5 ml of samples from the reservoir compartment was taken at a specified time interval, diluted appropriately, and the absorbance was measured spectrophotometrically at 263 nm. To maintain sink condition, the reservoir compartment was refilled every period with the same volume of fresh pH 7.4 phosphate buffer [30]. The amount of drug permeated by unit area has been calculated as a function of time. The flux was determined from the linear portion of the slope. The Rivastigmine Hydrogen Tartrate permeability coefficient (K_p) through porcine ear skin was determined using the relationship established from the first law of Fick's diffusion, represented in the following equation where "J is the flux and C is the concentration of drug in donor compartment" [31]:

$$K_p = J/C$$

Elasticity test - The deformability index is a unique parameter of transethosomal formulations as it differentiates transethosomes from liposomes and ethosomes that are unable to cross the intact stratum corneum. The elasticity of the prepared transethosomes, liposomes and ethosomes was measured by a technique called extrusion, through a polycarbonate membrane having a pore diameter of 200 nm, 25 mm diameter filters of 200 ml barrel capacity which was driven by an external pressure of 2.5 bars. The deformability index gives the measure of elasticity and was determined by using the following formula (32) where, D = Deformability index (ml/s), J = amount of suspension extruded (ml), t = extrusion time (s), r_v = vesicle size after extrusion (nm), r_p = pore size of the extrusion membrane (nm):

$$\mathbf{D = J/t\ (r_v/r_p)^2}$$

4.2.4. Formulation of patch incorporated with RHT-loaded transethosome

Preparation of backing layer - A 4% w/v PVA solution in water was prepared at 90˚C using a magnetic stirrer (Remi, 1MLH), 300 rpm for 30 minutes, and cast in a petri dish and placed in a 70˚C oven to eliminate any remaining solvent.

Preparation PSA matrix - Eudragit E100 as polymer, Dibutyl sebacate as a plasticizer, and Succinic acid as cross-linking agent are combined to make this matrix. According to the literature, the ratio of Eudragit E100, Dibutyl sebacate, and Succinic acid were 10:5:1 [33]. 1 g of Eudragit E100 was solubilised in 20 ml of Isopropyl Alcohol with the aid of a magnetic stirrer (Remi, 1MLH) at 300 rpm for 15 minutes. To this 0.1 g of Succinic acid was dissolved in small amounts of acetone and added. Further 0.5 ml of Dibutyl sebacate was added. Using 0.748% w/v of soya and 25.32% v/v of ethanol, optimised transethosomes were were prepared as derscribed in the method above. Finally, the transethosomal suspension equivalent to 4 mg of the drug (RHT) was added to the above mixture. The resulting solution was poured onto the backing layer contained in the Petri plate and the residual solvent was removed at 70˚C to obtain a dried film. Conventional patches were prepared by the above mentioned method, where the pure RHT was added instead of transethosomes.

4.2.5. Evaluation of patch incorporated with RHT-loaded transethosomes

Drug content - The transdermal patch of 1 cm^2 area was shredded and then transferred into a graduated flask containing 10 ml methanol and the flask was shaken constantly for 24 h. Then, using phosphate buffer pH 7.4, the entire solution was made up to 100 ml. following filtration, the amount of drug was measured using spectrophotometry at a wavelength of 263 nm [34].

Compatibility study of drug-excipient by FT-IR - The compatibility of the drug and the excipients was investigated using FT-IR spectroscopy. FT-IR spectra of Rivastigmine Hydrogen Tartrate and the final formulation were carried out by this technique to investigate the modifications in the chemical composition

of the drug after combining with excipients. The wave numbers of a characteristic peak of the formulation were compared with the pure drug and interpreted [4].

Ex vivo drug permeation studies of patches using porcine ear skin - A conventional patch containing pure drug (4 mg/ 2.25 cm^2) and a transethosomal patch of Rivastigmine Hydrogen Tartrate (4 mg/ 2.25 cm^2) were applied to the donor compartment on each dermal side of the skin respectively. The reservoir compartment had been loaded with 12 ml of pH 7.4 phosphate buffer comprising a small rotating magnetic bead at a steady 50 rpm speed. The study was performed for 24 h at 37± 0.5 ° C. At a fixed time period, 5 ml of sample was collected from the reservoir compartment. Which was suitably diluted and the absorbance was determined spectrophotometrically at 263 nm. Each period the reservoir compartment was replenished with the same amount of fresh pH 7.4 phosphate buffer in order to maintain sink conditions [30].

Skin deposition studies - The skin surface was cleansed five times with 5 ml of 30% methanol after the 24 h permeation experiment to eliminate excessive Rivastigmine Hydrogen Tartrate from the surface of the skin. Then the skin was cut into smaller fragments and added to 5 ml of 30% methanol followed by sonication for 10 minutes using ultrasonic probe sonicator (Sonics Vibra cell, CV18). The resulting solution was subjected to centrifugation for 15 minutes at 10,000 rpm. The supernatant was analysed for Rivastigmine Hydrogen Tartrate content by UV-visible spectrophotometer at 263 nm (10).

Acknowledgements: The authors thank the NGSM Institute of Pharmaceutical Sciences, Mangalore, for providing the necessary research facilities. The authors also thank STIC, Kochi, for performing SEM & TEM analysis.

Author contributions: Concept – C.L., S.P.; Design – C.L., S.P.; Supervision – S.P.; Resources – C.L., S.P.; Materials – C.L.; Data Collection and/or Processing – C.L.; Analysis and/or Interpretation – C.L., S.P.; Literature Search – C.L.; Writing – C.L.; Critical Reviews – C.L., S.P

Conflict of interest statement: The authors declared no conflict of interest.

REFERENCES

[1] Vijaykumar O, Joe VF, Vishwanath BA. Formulation and evaluation of rivastigmine loaded polymeric nanoparticles. J Chem Pharm Res. 2014;6(10):556–65. https://doi.org/10.1111/1523-1747.ep12497845

[2] Harilal S, Jose J, Parambi DGT, Kumar R, Mathew GE, Uddin MS, Kim H, Mathew B. Advancements in nanotherapeutics for Alzheimer's disease: current perspectives. Journal of Pharmacy and Pharmacology. 2019;71(9):1370-83. https://doi.org/10.1111/jphp.13132

[3] Sadowsky C, Perez JAD, Bouchard RW, Goodman I, Tekin S. Switching from oral cholinesterase inhibitors to the rivastigmine transdermal patch. CNS neuroscience & therapeutics. 16(1):51-60. https://doi.org/10.1111/j.1755-5949.2009.00119.x

[4] Sadeghi M, Ganji F, Taghizadeh SM, Daraei B. Preparation and characterization of rivastigmine transdermal patch based on chitosan microparticles. Iran J Pharm Res. 2016;15(3):283–94.

[5] Moretti DV, Frisoni GB, Giuliano B, Zanetti O. Comparison of the effects of transdermal and oral rivastigmine on cognitive function and EEG markers in patients with Alzheimer's disease. Front Aging Neurosci. 2014;6. https://doi.org/10.3389/fnagi.2014.00179

[6] Prabhakar D, Sreekanth J, Jayaveera KN. Transdermal Drug Delivery Patches: a Review. J Drug Deliv Ther. 2013;3(4). https://doi.org/10.22270/jddt.v3i4.590

[7] Arumugam K, Subramanian GS, Mallayasamy SR, Averineni RK, Reddy MS, Udupa N. A study of rivastigmine liposomes for delivery into the brain through intranasal route. Acta Pharm. 2008;58(3):287–97. https://doi.org/10.2478/v10007-008-0014-3

[8] Priya S, Lobo CL. Formulation and Optimization of Rivastigmine-Loaded PLGA and Chitosan Nanoparticles for Transdermal Delivery. Res J Pharm Technol. 2023;16(7):3175–82. https://doi.org/10.52711/0974-360X.2023.00522

[9] Chauhan MK, Sharma PK. Optimization and characterization of rivastigmine nanolipid carrier loaded transdermal patches for the treatment of dementia. Chem Phys Lipids. 2019;224. https://doi.org/10.1016/j.chemphyslip.2019.104794

[10] Shaji J, Bajaj R. Transethosomes: A New Prospect For Enhanced Transdermal Delivery. Int J Pharm Sci Res. 2018;9(7):2681–5. http://dx.doi.org/10.13040/IJPSR.0975-8232.9

[11] Müller T. Rivastigmine in the treatment of patients with Alzheimer's disease. Neuropsychiatr Dis Treat. 2007;3(2):211–18. https://doi.org/10.2147/nedt.2007.3.2.211

[12] Kumar L, Utreja P. Formulation and Characterization of Transethosomes for Enhanced Transdermal Delivery of

Propranolol Hydrochloride. Micro Nanosyst. 2019;12(1):38–47. https://doi.org/10.2174/1876402911666190603093550

[13] Kaur P, Garg V, Bawa P, Sharma R, Singh SK, Kumar B, Gulati M, Pandey NK, Narang R, Wadhwa S, Mohanta S, Jyoti J, Som S. Formulation, systematic optimization, in vitro, ex vivo, and stability assessment of transethosome based gel of curcumin. Asian J Pharm Clin Res. 2018;11(2):41-7. https://doi.org/10.22159/ajpcr.2018.v11s2.28563

[14] Garg V, Singh H, Bhatia A, Raza K, Singh SK, Singh B, Beg S. Systematic Development of Transethosomal Gel System of Piroxicam: Formulation Optimization, In Vitro Evaluation, and Ex Vivo Assessment. AAPS PharmSciTech. 2017;18(1):58–71. https://doi.org/10.1208/s12249-016-0489-z

[15] Albash R, Abdelbary AA, Refai H, El-Nabarawi MA. Use of transethosomes for enhancing the transdermal delivery of olmesartan medoxomil: In vitro, ex vivo, and in vivo evaluation. Int J Nanomedicine. 2019;14:1953–68. https://doi.org/10.2147/ijn.s196771

[16] Ascenso A, Raposo S, Batista C, Cardoso P, Mendes T, Praça FG, Bentley MV, Simões S. Development, characterization, and skin delivery studies of related ultradeformable vesicles: Transfersomes, ethosomes, and transethosomes. Int J Nanomedicine. 2015;10:5837–51. https://doi.org/10.2147/IJN.S86186

[17] Shaji J, Garude S. Transethosomes and Ethosomes for Enhanced Transdermal Delivery of Ketorolac Tromethamine: a Comparative Assessment. Int J Curr Pharm Res. 2014;6(4):88–93.

[18] Shaji J. Optimization and Characterization of 5-Fluorouracil Transethosomes for Skin Cancer Therapy Using Response Surface Methodology. Int J Adv Res. 2018;6(3):1225–33. http://dx.doi.org/10.21474/IJAR01/6789

[19] Kumar Mishra K, Deep Kaur C, Verma S, Kumar Sahu A, Kumar Dash D, Kashyap P, Prasad Mishra S. Transethosomes and Nanoethosomes: Recent Approach on Transdermal Drug Delivery System. In: Nanomedicines. 2019. http://dx.doi.org/10.5772/intechopen.81152.

[20] Allam AA, Fathalla D, Safwat MA, Soliman GM. Transferosomes versus transethosomes for the dermal delivery for minoxidil: Preparation and in vitro/ex vivo appraisal. J Drug Deliv Sci Technol. 2022;76. https://doi.org/10.1016/j.jddst.2022.103790

[21] Ansari MD, Ahmed S, Imam SS, Khan I, Singhal S, Sharma M, Sultana Y. CCD based development and characterization of nano-transethosome to augment the antidepressant effect of agomelatine on Swiss albino mice. J Drug Deliv Sci Technol. 2019;54:101234. https://doi.org/10.1016/j.jddst.2019.101234

[22] Fukuda IM, Pinto CFF, Moreira CDS, Saviano AM, Lourenço FR. Design of experiments (DoE) applied to pharmaceutical and analytical quality by design (QbD). Brazilian Journal of Pharmaceutical Sciences. 2018;54. https://doi.org/10.1590/s2175-97902018000001006

[23] Nayak D, Tawale RM, Aranjani JM, Tippavajhala VK. Formulation, Optimization and Evaluation of Novel Ultra-deformable Vesicular Drug Delivery System for an Anti-fungal Drug. AAPS PharmSciTech. 2020;21(5):1-10. https://doi.org/10.1208/s12249-020-01681-5

[24] Chen ZX, Li B, Liu T, Wang X, Zhu Y, Wang L, Wang XH, Niu X, Xiao Y, Sun Q. Evaluation of paeonol-loaded transethosomes as transdermal delivery carriers. Eur J Pharm Sci. 2017;99:240–5. https://doi.org/10.1016/j.ejps.2016.12.026

[25] Ma M, Wang J, Guo F, Lei M, Tan F, Li N. Development of nanovesicular systems for dermal imiquimod delivery: physicochemical characterization and in vitro/in vivo evaluation. J Mater Sci Mater Med. 2015;26(6);1-11. https://doi.org/10.1007/s10856-015-5524-1

[26] Habib BA, Sayed S, Elsayed GM. Enhanced transdermal delivery of ondansetron using nanovesicular systems: Fabrication, characterization, optimization and ex-vivo permeation study-Box-Cox transformation practical example. Eur J Pharm Sci. 2018;115:352–61. https://doi.org/10.1016/j.ejps.2018.01.044

[27] Malaiya MK, Jain A, Pooja H, Jain A, Jain D. Controlled delivery of rivastigmine using transdermal patch for effective management of alzheimer's disease. J Drug Deliv Sci Technol. 2018;45:408–14. https://doi.org/10.1016/j.jddst.2018.03.030

[28] Babita K, Kumar V, Rana V, Jain S, Tiwary A. Thermotropic and Spectroscopic Behavior of Skin: Relationship with Percutaneous Permeation Enhancement. Curr Drug Deliv. 2005;3(1):95–113. https://doi.org/10.2174/156720106775197466

[29] Smith WP, Christensen MS, Nacht S, Gans EH. Effect of lipids on the aggregation and permeability of human stratum corneum. J Invest Dermatol. 1982;78(1):7–11. https://doi.org/10.1111/1523-1747.ep12497845

[30] Nalluri BN, Prashanth Ram P, Chandra Teja U, Ashraf Sultana S. FORMULATION AND EVALUATION OF DRUG IN ADHESIVE TRANSDERMAL PATCHES OF RIVASTIGMINE. Indo Am J Pharm Res. 2014;4(11):5242-48.

[31] Ghanbarzadeh S, Arami S. Enhanced transdermal delivery of diclofenac sodium via conventional liposomes, ethosomes, and transfersomes. Biomed Res Int. 2013;2013. https://doi.org/10.1155/2013/616810

[32] Rady M, Gomaa I, Afifi N, Abdel-Kader M. Dermal delivery of Fe-chlorophyllin via ultradeformable nanovesicles for photodynamic therapy in melanoma animal model. Int J Pharm. 2018;548(1):480–90. https://doi.org/10.1016/j.ijpharm.2018.06.057

[33] Hu Y, Wu YY, Xia XJ, Wu Z, Liang WQ, Gao JQ. Development of drug-in-adhesive transdermal patch for α-asarone and in vivo pharmacokinetics and efficacy evaluation. Drug Deliv. 2011;18(1):84–9. https://doi.org/10.3109/10717544.2010.520350

[34] Parhi R, Padilam S. In vitro permeation and stability studies on developed drug-in-adhesive transdermal patch of simvastatin. Bull Fac Pharmacy, Cairo Univ. 2018;56(1):26–33. https://doi.org/10.1016/j.bfopcu.2018.04.001